



# Recurrent *KRAS* mutations in papillary renal neoplasm with reverse polarity

Khaleel I. Al-Obaidy<sup>1</sup> · John N. Eble<sup>1</sup> · Mehdi Nassiri<sup>1</sup> · Liang Cheng<sup>1</sup> · Mohammad K. Eldomery<sup>1</sup> · Sean R. Williamson<sup>2</sup> · Wael A. Sakr<sup>3</sup> · Nilesh Gupta<sup>2</sup> · Oudai Hassan<sup>2</sup> · Muhammad T. Idrees<sup>1</sup> · David J. Grignon<sup>1</sup>

Received: 5 August 2019 / Revised: 22 August 2019 / Accepted: 23 August 2019 / Published online: 18 September 2019  
© United States & Canadian Academy of Pathology 2019

## Abstract

We recently proposed that an epithelial renal tumor “papillary renal neoplasm with reverse polarity” represents a distinct entity. It constituted 4% of previously diagnosed papillary renal cell carcinoma at the participating institutions. Histologically, it is characterized by papillary or tubulopapillary architecture covered by a single layer of eosinophilic cells with finely granular cytoplasm and apically located nuclei. It is characteristically positive for GATA3 and L1CAM and lack vimentin and, to a lesser extent,  $\alpha$ -methylacyl-CoA-racemase (AMACR/p504s) immunostaining. To investigate the molecular pathogenesis of these tumors, we performed targeted next-generation sequencing on ten previously reported papillary renal neoplasms with reverse polarity, followed by a targeted polymerase chain reaction analysis for *KRAS* mutations in a control series of 30 type 1 and 2 papillary renal cell carcinomas. *KRAS* missense mutations were identified in eight of ten papillary renal neoplasms with reverse polarity. These mutations were clustered in exon 2—codon 12: c.35 G > T ( $n = 6$ ) or c.34 G > C ( $n = 2$ ) resulting in p.Gly12Val and p.Gly12Arg alterations, respectively. One of the wild-type tumors had *BRAF* c.1798\_1799delGTinsAG (p.Val600Arg) mutation. No *KRAS* mutations were identified in any of the 30 control tumors. In summary, this study supports our proposal that papillary renal neoplasm with reverse polarity is an entity distinct from papillary renal cell carcinoma and the only renal cell neoplasm to consistently harbor *KRAS* mutations.

## Introduction

In 1997, Delahunt and Eble proposed that papillary renal cell carcinoma could be classified into types 1 and 2 [1]. Results of the Cancer Genome Atlas (TCGA) molecular characterization have supported this histologic classification. However, the observed histologic heterogeneity of papillary renal cell carcinoma type 2 is also reflected on a molecular level as

indicated by several studies [2–5]. Type 1 tumors are associated with *MET* alterations, whereas type 2 tumors consist of at least three subtypes based on molecular features and are characterized by *CDKN2A* silencing, *SETD2* mutations, *TFE3* fusions, and increased expression of the NRF2–antioxidant response element pathway [4]. Ultimately, these advances in genetic understanding have led to the recognition of distinct tumor entities that were once included under the umbrella of papillary renal cell carcinoma type 2, including for instance hereditary leiomyomatosis and renal cell carcinoma syndrome-associated renal cell carcinoma and some translocation carcinomas [6].

We recently described a subset of papillary renal neoplasms and proposed the term papillary renal neoplasm with reverse polarity [7]. This tumor was found equally in men and women, with a median age of 66 years. All 18 tumors were  $\leq 3$  cm in size (median 1.4 cm, mean 1.6 cm) and ten were encapsulated. All tumors were low stage and appear to have been cured by surgery. Microscopically, the tumors were composed of papillary or tubulopapillary architecture covered by a single layer of eosinophilic cells with finely granular eosinophilic cytoplasm and apically located round

**Supplementary information** The online version of this article (<https://doi.org/10.1038/s41379-019-0362-1>) contains supplementary material, which is available to authorized users.

✉ John N. Eble  
jeble@iupui.edu

- <sup>1</sup> Department of Pathology and Laboratory Medicine, Indiana University School of Medicine, Indianapolis, IN, USA
- <sup>2</sup> Department of Pathology and Laboratory Medicine, Henry Ford Health System, Detroit, MI, USA
- <sup>3</sup> Department of Pathology and Laboratory Medicine, Wayne State University/Harper University Hospital, Detroit, MI, USA

nuclei with inconspicuous nucleoli. No intracellular hemosiderin, psammoma bodies, mitotic figures, necrosis, or clusters of foamy macrophages were seen. The diagnosis was aided by positive immunohistochemical staining for GATA3 and L1CAM along with the lack of vimentin and, to a lesser extent,  $\alpha$ -methylacyl-CoA-racemase (AMACR/p504s) staining. Fluorescence in situ hybridization analysis demonstrated a lower level of chromosomal abnormalities (chromosome 7 and 17 trisomy in 20% of tumors and deletion of Y chromosome in 14% of the tumors in males). These findings are largely atypical for papillary renal cell carcinomas types 1 and 2 [7].

In the current study, we performed mutational analysis of the papillary renal neoplasm with reverse polarity using a targeted next-generation sequencing (NGS) platform and report a novel recurrent genetic mutation in these tumors.

## Materials and methods

### Study population

The study was approved by the Institutional Review Board of the participating institutions (Indiana University, Indianapolis, IN; Henry Ford Health System, Detroit, MI; and Wayne State University, Detroit, MI). Based on availability of sufficient material for molecular analysis, the study included ten of the previously published tumors of papillary renal neoplasm with reverse polarity obtained from the three departments of pathology (corresponding tumors no. 2, 4, 5, 8, 10, 11, 12, 14, 15, and 17). As previously described, a control group composed of 30 papillary renal cell carcinomas (15 tumors of type 1 and 15 tumors of type 2) was selected from the archives of the participating institutions. To be selected for the control group, the tumors were reviewed independently by two pathologists (DJG and JNE). Both were blinded to the initial diagnosis and each other's diagnosis. Only tumors where classification into types 1 and 2 was in agreement were then utilized as controls. All tumors had been fixed in 10% neutral-buffered formalin and embedded in paraffin [7].

### NGS and mutational analysis

Representative formalin-fixed, paraffin-embedded blocks of ten papillary renal neoplasms with reverse polarity containing more than 60% tumor were submitted for targeted NGS using the University of Chicago Medicine OncoPlus (UCM-OncoPlus) panel, a hybrid-capture panel targeting 1213 cancer-associated genes. DNA extraction, DNA quantification, library preparation, and sequencing were performed as previously described [8]. Data analysis was performed on a compliant high-performance computing

system (Center for Research Informatics, University of Chicago) using a University of Chicago developed bioinformatics pipeline. First, using Novoalign 3.02.07 (NovoCraft, Selangor, Malaysia), the data were aligned to the hg19 reference human genome. Then, Samtools 0.1.1915 mpileup and Variant Inspector version 1.0, an UCM-developed variant calling software, were used for variant calling. Subsequently, variants were filtered based on depth ( $>100\times$ ), Phred quality score ( $>30$ ), minor allele frequency (MAF  $>5\%$ ), and location in clinical exonic territory for review. Variant calls were annotated and converted to Human Genome Variation Society nomenclature using Alamut Batch version 1.3.0 software. Further manual variant curation was followed in accordance with the Association for Molecular Pathology recommendations [9].

### KRAS mutational analysis

Based on the NGS findings, a targeted polymerase chain reaction analysis was performed on the control tumors as previously described [10]. Briefly, formalin-fixed, paraffin-embedded tissue blocks were retrieved from each control tumor. DNA extraction from each block was performed using the Qiagen QIAamp DNA FFPE Tissue Kit (Qiagen, Valencia, CA, USA). DNA concentration was determined using the NanoDrop Spectrophotometer and adjusted to  $\sim 10$  ng/ $\mu$ l in ddH<sub>2</sub>O. Polymerase chain reaction testing was performed according to the recommended procedure using the Qiagen therascreen *KRAS* RGQ PCR Kit on the Qiagen Rotor-Gene Q MDx instrument. The therascreen *KRAS* RGQ PCR Kit provides eight separate PCR amplification reactions: seven mutation-specific reactions in codons 12 and 13 of exon 2 of the *KRAS* oncogene [Gly12Ala (G12A), Gly12Asp (G12D), Gly12Arg (G12R), Gly12Cys (G12C), Gly12Ser (G12S), Gly12Val (G12V), and Gly13Asp (G13D)] and a wild-type control in exon 4. Analysis of crossing thresholds and mutation calls for each PCR amplification reaction were performed by the Rotor-Gene Q therascreen *KRAS* Assay analysis software once runs were completed.

### Evaluation of TCGA renal neoplasms data for gene expression

Data of the mRNA expression (mRNA seqV2, RSEM normalized values) of a cohort of 17 tumors obtained from TCGA (Kidney renal papillary cell carcinoma "KIRP" project) were utilized for mRNA clustering analysis using 20531 gene signatures. The tumors were divided into four groups based on the *KRAS* mutational status and the histologic criteria, as defined by Delahunt and Eble [1], using the digital images available at TCGA website. These groups included: three papillary renal neoplasms with

**Table 1** Clinical, pathological, and molecular characteristics of selected papillary renal neoplasm with reverse polarity tumors

Case no.	Procedure	Gender	Age (years)	Size (mm)	Encapsulated	pT-category	WHO/ISUP nuclear grade	Gene mutation	Minor allele frequency	Follow-up period (months)	Recurrence/ Metastasis
1	Partial nephrectomy	Female	75	10	No	pT1a	2	<i>KRAS</i> p.Gly12Val <i>BRCA2</i> p.Trp1692Metfs	13%	44	No
2	Partial nephrectomy	Male	69	10	No	pT1a	2	<i>KRAS</i> p.Gly12Arg	34%	16	No
3	Total nephrectomy	Female	77	10	Yes	pT1a	2	<i>KRAS</i> p.Gly12Val <i>TP53</i> p.Arg213Gln	20%	30	No
4	Total nephrectomy	Male	66	10	Yes	pT1a	1	<i>KRAS</i> p.Gly12Val	14%	80	No
5	Total nephrectomy	Female	58	11	Yes	pT1a	1	<i>KRAS</i> p.Gly12Val	28%	1	No
6	Partial nephrectomy	Female	46	30	No	pT1a	1	<i>KRAS</i> p.Gly12Val	34%	1	No
7	Partial nephrectomy	Male	66	30	Yes	pT1a	2	<i>KRAS</i> p.Gly12Val	25%	17	No
8	Total nephrectomy	Male	75	8	Yes	pT1a	2	<i>KRAS</i> p.Gly12Arg <i>BRCA2</i> p.Val2610Met	29%	7	No
9	Partial nephrectomy	Male	50	11	Yes	pT1a	2	<i>BRAF</i> p.Val600Arg	30%	22	No
10	Total nephrectomy	Female	70	12	Yes	pT1a	2	No pathogenic mutations		–	No additional follow-up

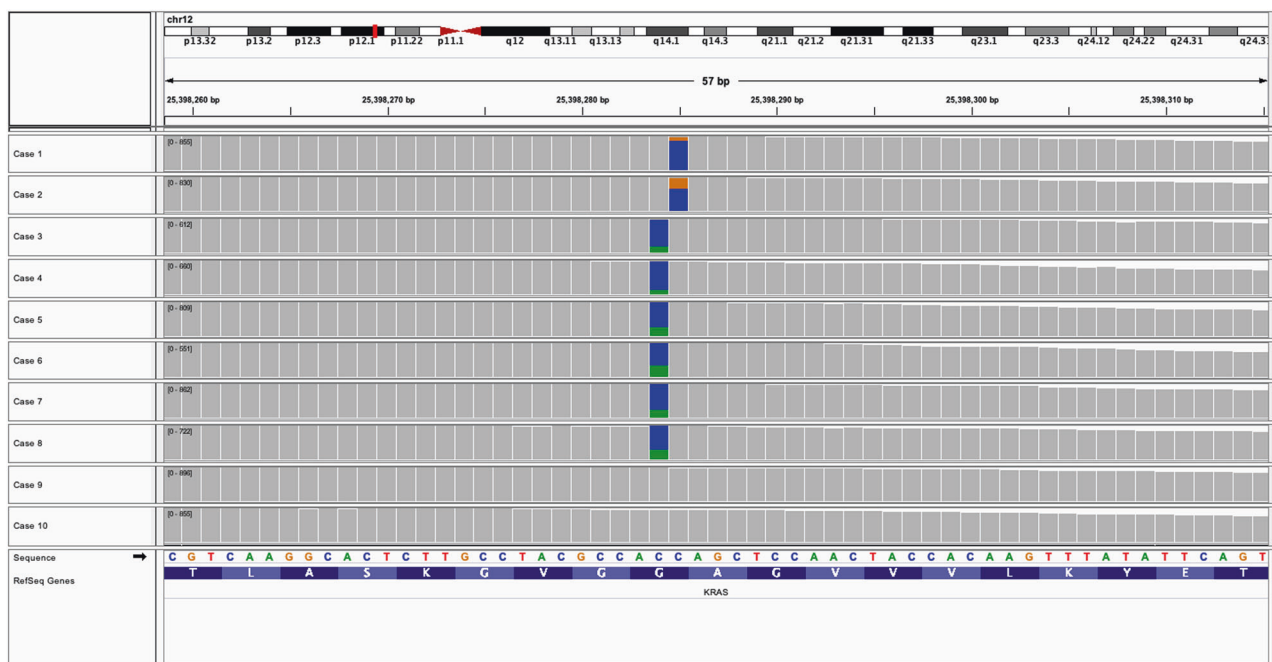


**Fig. 1** Integrative Genomics Viewer snapshot of human *KRAS* gene with the location of the missense mutations identified in eight papillary renal neoplasms with reverse polarity tumors. The mutations are all

reverse polarity (TCGA-2Z-A9JN, TCGA-BQ-5883, and TCGA-A4-8312), two *KRAS* mutated papillary renal cell carcinomas (TCGA-GL-A9DC and TCGA-MH-A854), six papillary renal cell carcinomas type 1 (TCGA-2Z-A9J6, TCGA-2Z-A9JE, TCGA-2Z-A9JL, TCGA-2Z-A9JZ, TCGA-2Z-A9K0, and TCGA-SX-A71S), and six papillary renal cell carcinomas type 2 (TCGA-2Z-A9J2, TCGA-2Z-A9JD, TCGA-5P-A9JW, TCGA-B9-A8YI, TCGA-B9-A44B, and TCGA-IA-A83S).

Unsupervised clustering analysis of the 17 tumors was performed using the GENE-E software (<https://software.broadinstitute.org/GENE-E/index.html/>) and Genesis platform (Graz, Austria) [11]. K-mean clustering with average linkage of Euclidian distance for both samples and genes was performed. Same set of samples was analyzed in Firebrowse portal (<http://www.firebrowse.org/>).

## Results

NGS was performed on DNA isolated from ten papillary renal neoplasms with reverse polarity as described in the section “Materials and methods.” The clinicopathologic and mutational results are summarized in Table 1 and Supplementary Table 1. Bioinformatics analysis revealed recurrent missense mutations in the *KRAS* (NM\_033360.3) in eight tumors (80%). These mutations were due to either a c.35 G>T ( $n=6$ ) or c.34 G>C ( $n=2$ ) substitution, resulting in p.Gly12Val and p.Gly12Arg alterations,

clustered within two recurrent hotspots (p.Gly12Val and p.Gly12Arg). Blue denotes T-nucleotide (normal), green denotes A-nucleotide (p.Gly12Val), and orange denotes G-nucleotide (p.Gly12Arg)

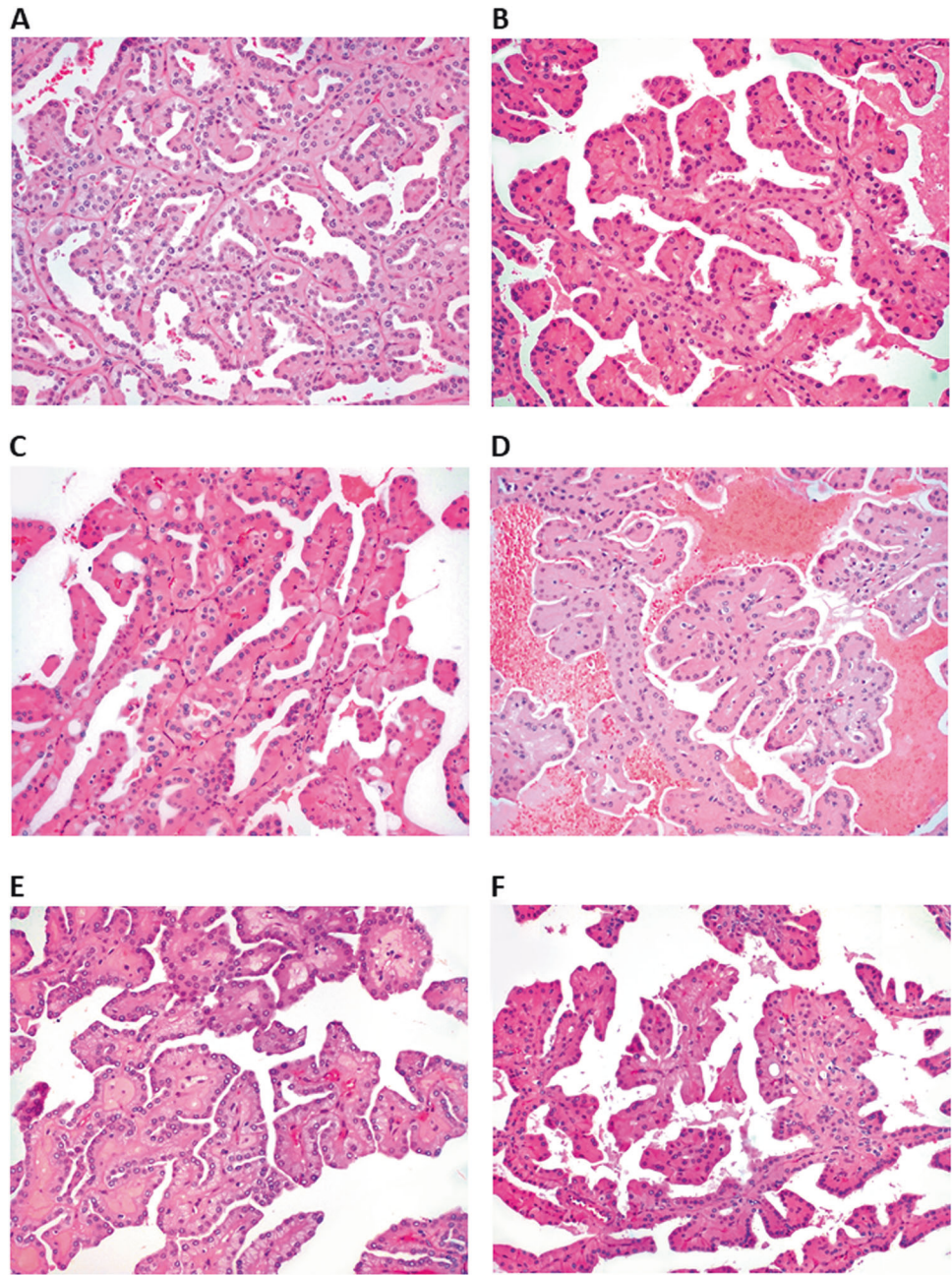


**Fig. 2** Next-generation sequencing results on ten papillary renal neoplasms with reverse polarity tumors. *KRAS* mutation and other somatic mutations identified are shown

respectively (Fig. 1). The minor allele frequency ranged from 13–34%, supporting the somatic origin. Both of these variants are common somatic mutations in cancer and have been classified as pathogenic in the Catalogue of Somatic Mutations in Cancer (COSMIC) and ClinVar databases [12, 13].

Targeted NGS also revealed mutations in *TP53*, *BRCA2*, and *BRAF* in tumors no. 3, 8, and 9, respectively, and duplication in *BRCA2* in tumor no. 1 (Fig. 2). *BRCA2* is a tumor suppressor gene and is known to predispose patients to breast and ovarian carcinoma [14, 15]. A frameshift duplication c.5073dup (p.Trp1692Metfs\*3) and missense mutations c.4258 G>T (p.Asp1420Tyr) were identified in the *BRCA2* gene (NM\_000059.3) in two tumors (no. 1 and 8, respectively). Both have been reported as pathogenic somatic mutations in cancer (COSMIC v89) [16, 17]. Tumor no. 3 harbored missense mutation in the *TP53* (NM\_000546.5) tumor suppressor gene c.638 G>A (p.Arg213Gln). This mutation is recurrent in many sporadic and familial tumors

**Fig. 3** Representative histologic images of papillary renal neoplasms with reverse polarity. All formed thin papillary architecture with delicate fibrovascular cores with variable proportion of tubular formation. The cells are mostly cuboidal with eosinophilic, finely granular cytoplasm and the nuclei are characteristically located at the apical surface of the cells. Nuclei are mostly small, nonoverlapping with regular nuclear contours, occasional nuclear clearing, and inconspicuous nucleoli.  
**a, b** *KRAS* and *BRCA1* mutated (tumor no. 8) or *BRCA1* duplicated (tumor no. 1).  
**c** *KRAS* only mutated (tumor no. 2). **d** *KRAS* and *TP53* mutated (tumor no. 3). **e** *BRAF* mutated (tumor no. 9). **f** *KRAS* wild type (tumor no. 10)



[18]. Lastly, one tumor (no. 9) carried *BRAF* (NM\_004333) c.1798\_1799delGTinsAG (p.Val600Arg) mutation, which is reported in melanoma, colorectal, and pancreatic carcinoma (COSM474) [16, 17]. This tumor lacked *KRAS* mutation. *BRAF* protein is a downstream effector in the *KRAS* pathway and the mutual exclusivity of these two mutations has been suggested by some researchers [19, 20]. Representative histologic images of the analyzed tumors are shown in Fig. 3.

We performed a targeted polymerase chain reaction analysis of the 30 papillary renal cell carcinomas in the control group and found no hotspot mutations in the *KRAS* in any of them.

To further validate our findings, we examined the publicly available database in TCGA (KIRP project) and found five tumors with *KRAS* mutations. Three of the five were papillary renal neoplasms with reverse polarity (TCGA-2Z-A9JN, TCGA-A4-8312, and TCGA-BQ-5883) based on the available digital images (Figs. 4 and 5). All of these had *KRAS* mutations in the same hotspots (c.35 G > T and c.34 G > C) found in our tumors. Interestingly, the mutational burden of the three tumors was low ( $\leq 20$  mutations), with *KRAS* being the only shared mutation among them. All three tumors were reported as diploid.

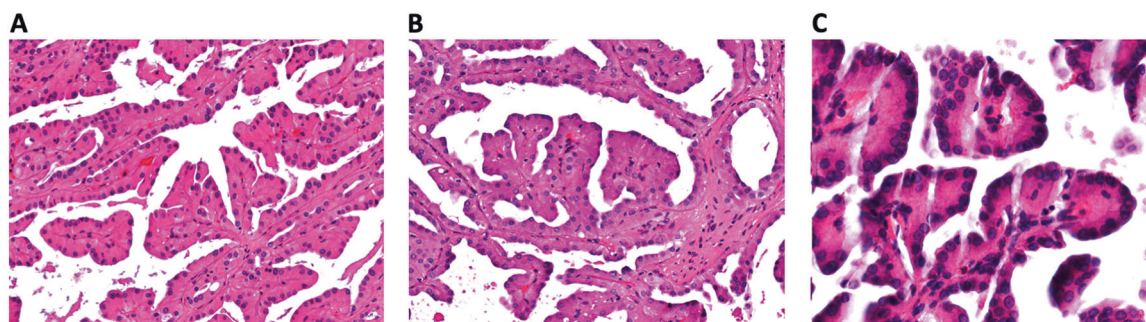
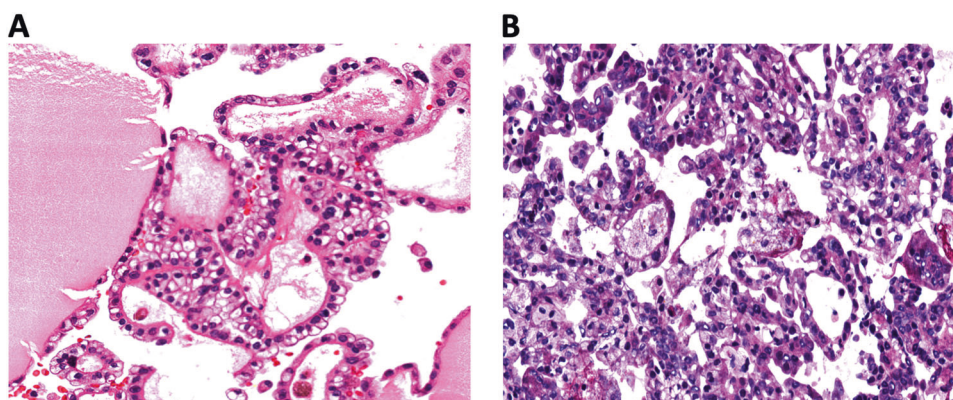


**Fig. 4 a, b, c** The Cancer Genome Atlas histologic images of the three papillary renal neoplasms with reverse polarity tumors harboring *KRAS* mutation [(TCGA-2Z-A9JN, TCGA-BQ-5883, and TCGA-A4-8312, respectively), <https://portal.gdc.cancer.gov/projects/TCGA-KIRP>]

**Fig. 5 a, b** The Cancer Genome Atlas histologic images of the two *KRAS* mutated papillary renal cell carcinomas, type 1 [(TCGA-GL-A9DC and TCGA-MH-A854, respectively), <https://portal.gdc.cancer.gov/projects/TCGA-KIRP>]



Unsupervised mRNA clustering of the 17 Cancer Genome Atlas tumors (three papillary renal neoplasms with reverse polarity, two *KRAS* mutated papillary renal cell carcinomas, six papillary renal cell carcinomas type 1, and six papillary renal cell carcinomas type 2) showed papillary renal neoplasms with reverse polarity to have a different expression profile compared with other groups (Fig. 6), further supporting our analysis.

## Discussion

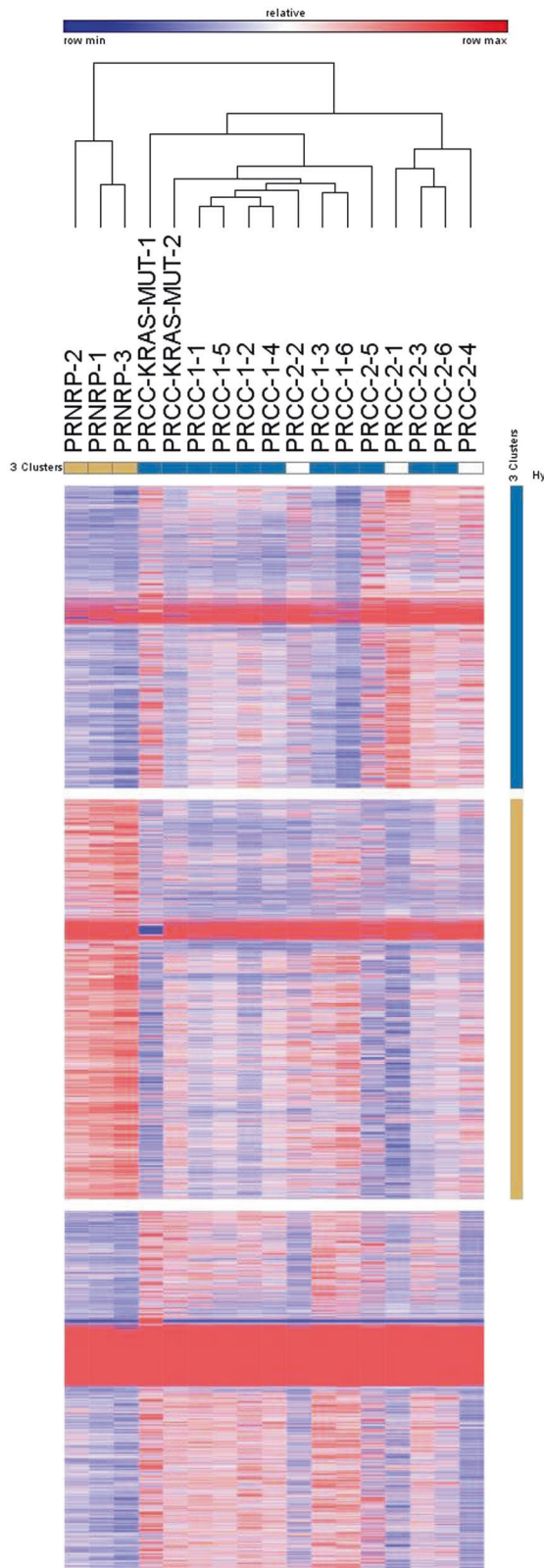
This study identifies for the first time a renal cell neoplasm with consistent *KRAS* mutations. In addition to our previous report of the distinct morphologic, immunohistochemical, and chromosomal features of papillary renal neoplasm with reverse polarity, this study also shows a recurrent pathogenic mutation that is distinct from any previously found in renal cell neoplasms, including papillary renal cell carcinoma types 1 and 2.

*KRAS* proto-oncogene, GTPase is part of the RAS family. It encodes GTPase enzyme that functions as molecular regulator of proliferation and cell survival pathways [21]. Abnormal function of *KRAS* is associated with tumorigenesis and typically arises from single mutation at

codons 12, 13, or 61, which leads to constitutive activation of the gene [22].

In addition to papillary renal neoplasm with reverse polarity, the COSMIC v89 shows *KRAS* mutation in a number of cancers, including pancreatic, colorectal, and lung adenocarcinomas. *KRAS* mutations are also reported in benign lesions, although to a much lesser extent than cancers, including papillary fibroelastoma, ovarian mucinous cystadenoma, and intracranial arteriovenous malformations [10, 23, 24]. In the kidney, it accounts for only a minority (0.8%,  $n = 33/4207$ ) of mutations reported in COSMIC (Supplementary Table 2). Five (5/33) of these tumors were reported as papillary renal cell carcinomas, two of which are papillary renal neoplasms with reverse polarity as determined by examining the available digital histologic images (TCGA-BQ-5883-01 and TCGA-A4-8312-01). Of note, one of the studies that were cited in COSMIC v89 reported *KRAS* mutations in 100% of clear cell renal cell carcinomas ( $n = 11$ ) [25]. These results have not been reproduced by larger studies including TCGA database where only 0.1% of clear cell renal cell carcinomas had a *KRAS* mutation,  $n = 1/537$  in the kidney renal clear cell carcinoma project.

In a report by Saleeb et al., a partial molecular overlap between tumors similar to papillary renal neoplasm with reverse polarity and papillary renal cell carcinoma type 2



◀ **Fig. 6** Unsupervised mRNA clustering analysis of 17 tumors obtained from the Cancer Genome Atlas database [three papillary renal neoplasms with reverse polarity (PRNRP), two *KRAS* mutated papillary renal cell carcinomas (PRCC-KRAS-MUT), six papillary renal cell carcinomas type 1 (PRCC-1), and six papillary renal cell carcinomas type 2 (PRCC-2)] using 20531 genes. Papillary renal neoplasm with reverse polarity tumors cluster together in a distinct group. The clusters shown are based on K-mean method (GENE-E) with average linkage of Euclidian distance for both samples and genes. Blue denotes upregulated genes and red denotes downregulated genes

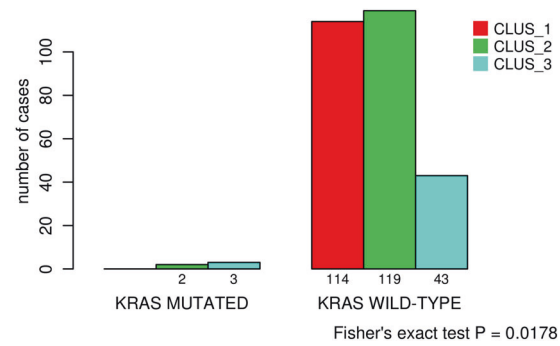


**Fig. 7** *KRAS* mutation status versus mRNA Seq hierarchical from Firebrowse portal. The three papillary renal neoplasms with reverse polarity tumors are clustered into distinct cluster than other *KRAS* mutated tumors. Broad Institute TCGA Genome Data Analysis Center (2016): correlation between gene mutation status and molecular subtypes. Broad Institute of MIT and Harvard. doi:10.7908/C1PN9526

was found, where papillary renal cell carcinoma type 2 had additional unique pathways associated with tumor aggressiveness and metastasis. However, when clustering analysis

was performed, papillary renal neoplasm with reverse polarity tumors had its own distinct molecular cluster with minimal overlap with papillary renal cell carcinoma type 2 [3]. Further, similar clusters were found based on *KRAS* mutational status of the same Cancer Genome Atlas tumors in Firebrowse portal (Fig. 7).

The shared characteristic location of the nuclei away from the basement membrane is a unique feature, which has been described in only a few tumors, including tall cell carcinoma (solid papillary carcinoma) with reverse polarity of the breast. Chiang et al. were the first to describe a unique *IDH2* or *PIK3CA* mutation in these tumors [26]. However, mutations in those two genes were not identified in our tumors, suggesting that another driving genes responsible for the reverse polarity phenotype.

In summary, the identification of consistent pathogenic *KRAS* mutations in papillary renal neoplasm with reverse polarity provides further evidence of the distinct nature of this entity. Although further studies with a larger series of tumors are recommended, the finding of *KRAS* mutation is two separate, unrelated cohorts (ours and TCGA), which supports our proposal that this morphologic entity is a result of a molecular pathogenic process different from other renal cell neoplasms. Our study provides the evidence for the first renal cell neoplasm characterized by *KRAS* mutation.

## Compliance with ethical standards

**Conflict of interest** The authors declare that they have no conflict of interest.

**Publisher's note** Springer Nature remains neutral with regard to jurisdictional claims in published maps and institutional affiliations.

## References

- Delahunt B, Eble JN. Papillary renal cell carcinoma: a clinicopathologic and immunohistochemical study of 105 tumors. *Mod Pathol.* 1997;10:537–44.
- Marsaud A, Dadone B, Ambrosetti D, Baudoin C, Chamorey E, Rouleau E, et al. Dismantling papillary renal cell carcinoma classification: the heterogeneity of genetic profiles suggests several independent diseases. *Genes Chromosomes Cancer.* 2015;54:369–82.
- Saleeb RM, Brimo F, Farag M, Rompre-Brodeur A, Rotondo F, Beharry V, et al. Toward biological subtyping of papillary renal cell carcinoma with clinical implications through histologic, immunohistochemical, and molecular analysis. *Am J Surg Pathol.* 2017;41:1618–29.
- Linehan WM, Spellman PT, Ricketts CJ, Creighton CJ, Fei SS, Cancer Genome Atlas Research Network, et al. Comprehensive molecular characterization of papillary renal-cell carcinoma. *N Engl J Med.* 2016;374:135–45.
- Saleeb RM, Plant P, Tawedrous E, Krizova A, Brimo F, Evans AJ, et al. Integrated phenotypic/genotypic analysis of papillary renal cell carcinoma subtypes: identification of prognostic markers, cancer-related pathways, and implications for therapy. *Eur Urol Focus.* 2018;4:740–8.
- Strigley JR, Delahunt B, Eble JN, Egevad L, Epstein JI, Grignon D, et al. The International Society of Urological Pathology (ISUP) Vancouver classification of renal neoplasia. *Am J Surg Pathol.* 2013;37:1469–89.
- Al-Obaidy KI, Eble JN, Cheng L, Williamson SR, Sakr WA, Gupta N, et al. Papillary renal neoplasm with reverse polarity: a morphologic, immunohistochemical, and molecular study. *Am J Surg Pathol.* 2019;43:1099–111.
- Parilla M, Alikhan M, Al-Kawaaz M, Patil S, Kadri S, Ritterhouse LL, et al. Genetic underpinnings of renal cell carcinoma with leiomyomatous stroma. *Am J Surg Pathol.* 2019;43:1135–44.
- Li MM, Datto M, Duncavage EJ, Kulkarni S, Lindeman NI, Roy S, et al. Standards and guidelines for the interpretation and reporting of sequence variants in cancer: a joint consensus recommendation of the Association for Molecular Pathology, American Society of Clinical Oncology, and College of American Pathologists. *J Mol Diagn.* 2017;19:4–23.
- Priemer DS, Vortmeyer AO, Zhang S, Chang HY, Curless KL, Cheng L. Activating *KRAS* mutations in arteriovenous malformations of the brain: frequency and clinicopathologic correlation. *Hum Pathol.* 2019;19:33–9.
- Sturn A, Quackenbush J, Trajanoski Z. Genesis: cluster analysis of microarray data. *Bioinformatics.* 2002;18:207–8.
- Forbes SA, Beare D, Boutselakis H, Bamford S, Bindal N, Tate J, et al. COSMIC: somatic cancer genetics at high-resolution. *Nucleic Acids Res.* 2017;45:D777–83.
- Landrum MJ, Lee JM, Benson M, Brown GR, Chao C, Chitipiralla S, et al. ClinVar: improving access to variant interpretations and supporting evidence. *Nucleic Acids Res.* 2018;46:D1062–67.
- Antoniou AC, Pharoah PD, McMullan G, Day NE, Ponder BA, Easton D. Evidence for further breast cancer susceptibility genes in addition to *BRCA1* and *BRCA2* in a population-based study. *Genet Epidemiol.* 2001;21:1–18.
- Risch HA, McLaughlin JR, Cole DE, Rosen B, Bradley L, Kwan E, et al. Prevalence and penetrance of germline *BRCA1* and *BRCA2* mutations in a population series of 649 women with ovarian cancer. *Am J Hum Genet.* 2001;68:700–10.
- Dutton-Regester K, Kakavand H, Aoude LG, Stark MS, Gartside MG, Johansson P, et al. Melanomas of unknown primary have a mutation profile consistent with cutaneous sun-exposed melanoma. *Pigment Cell Melanoma Res.* 2013;26:852–60.
- Zhu XL, Cai X, Zhang L, Yang F, Sheng WQ, Lu YM, et al. [*KRAS* and *BRAF* gene mutations in correlation with clinicopathologic features of colorectal carcinoma in Chinese]. *Zhonghua Bing Li Xue Za Zhi* 2012;41:584–9.
- Chang MT, Asthana S, Gao SP, Lee BH, Chapman JS, Kandath C, et al. Identifying recurrent mutations in cancer reveals widespread lineage diversity and mutational specificity. *Nat Biotechnol.* 2016;34:155–63.
- Davies H, Bignell GR, Cox C, Stephens P, Edkins S, Clegg S, et al. Mutations of the *BRAF* gene in human cancer. *Nature.* 2002;417:949–54.
- Oikonomou E, Koustas E, Goulielmaki M, Pintzas A. *BRAF* vs *RAS* oncogenes: are mutations of the same pathway equal? Differential signalling and therapeutic implications. *Oncotarget.* 2014;5:11752–77.
- Quinlan MP, Settleman J. Isoform-specific *ras* functions in development and cancer. *Future Oncol.* 2009;5:105–16.
- Prior IA, Lewis PD, Mattos C. A comprehensive survey of *Ras* mutations in cancer. *Cancer Res.* 2012;72:2457–67.
- Wittersheim M, Heydt C, Hoffmann F, Buttner R. *KRAS* mutation in papillary fibroelastoma: a true cardiac neoplasm? *J Pathol Clin Res.* 2017;3:100–4.
- Lee YJ, Lee MY, Ruan A, Chen CK, Liu HP, Wang CJ, et al. Multipoint *Kras* oncogene mutations potentially indicate mucinous carcinoma on the entire spectrum of mucinous ovarian neoplasms. *Oncotarget.* 2016;7:82097–103.
- Raspolini MR, Castiglione F, Martignoni G, Cheng L, Montironi R, Lopez-Beltran A. Unlike in clear cell renal cell carcinoma, *KRAS* is not mutated in multilocular cystic clear cell renal cell neoplasm of low potential. *Virchows Arch.* 2015;467:687–93.
- Chiang S, Weigelt B, Wen HC, Pareja F, Raghavendra A, Martelotto LG, et al. *IDH2* mutations define a unique subtype of breast cancer with altered nuclear polarity. *Cancer Res.* 2016;76:7118–29.